Discovery of novel anti-leishmanial agents targeting LdLip3 lipase

Saravanan Parameswaran, Prakash Saudagar, Vikash Kumar Dubey, Sanjukta Patra *

Department of Biotechnology, Indian Institute of Technology Guwahati, Guwahati 781039, Assam, India

ARTICLE INFO

ABSTRACT

Leishmaniasis is a neglected tropical disease, caused by several species of *Leishmania*. Being an opportunistic lipid-scavenging pathogen, *Leishmania* relies extensively on lipid metabolism especially for host–pathogen interaction, utilizing host lipids for energy and virulence. The rational approach is to target lipid metabolism of the pathogen focusing lipid-catabolizing lipases. The LdLip3 lipase is considered as drug target as it is constitutively expressed in both promastigote and amastigote forms. Since the LdLip3 structure is not known, we modeled its three-dimensional structure to implement structure-based drug discovery approach. Similarity-based virtual screening was carried out to identify potential inhibitors utilizing NCI diversity set on ZINC database including natural products. Implementing computational and experimental approaches, four anti-leishmanial agents were discovered. The screened molecules ZINC01821375, ZINC04008765, ZINC06117316 and ZINC12653571 had anti-leishmanial activity with IC_{50} (% viable promastigotes *vs.* concentration) of $5.2 \pm 1.8 \, \mu M$, $13.1 \pm 2.6 \, \mu M$, $9.4 \pm 2.6 \, \mu M$ and $17.3 \pm 3.1 \, \mu M$, respectively. The molecules showed negligible toxicity toward mouse macrophages. Based on the contact footprinting analysis, new molecules were designed with better predicted free energy of binding than discovered anti-leishmanial agents. Further validation for the therapeutic utility of discovered molecules can be carried out by the research community to combat leishmaniasis.

© 2014 Elsevier Inc. All rights reserved.

1. Introduction

Leishmaniasis is considered as an emerging disease with about 12 million infected people worldwide [1]. Several species and sub-species of *Leishmania*, an intra-macrophage obligate parasite causes clinically heterogeneous leishmaniasis. The fatal visceral leishmaniasis is linked with *Leishmania donovani*, *L. infantum* and *L. chagasi*. *L. donovani* is predominant in India [2,3]. Leishmaniasis is widespread in 98 countries with 350 million people at risk. Unfortunately, it has been underreported for several decades and still has a neglected status [4,5]. The available therapeutics is associated with high toxicity, high cost and low efficacy (Supplementary Table 1) [6,7]. Emergence of HIV coinfection, drug-resistance and disease spreading worldwide worsens the current scenario that urges the need for new/novel drugs to combat leishmaniasis. Few research organizations stress on the control measures along with the identification of new drug targets and drugs [8,9].

Leishmania is a lipid-scavenging pathogen with dimorphic life cycle. The parasite is transmitted into mammalian host by female phlebotomine sand flies and it relies highly on its lipid metabolism to survive in different milieu of the hosts [10]. The lipid metabolism of pathogen plays a vital role in energy storage and pathogenesis [11]. Additional roles of the lipid metabolism have been implicated in cellular signaling as well as organization, dynamics and trafficking of membrane [12]. The systemic metabolic analysis in *Leishmania major* revealed that (i) most of the intracellular reactions participate in lipid metabolism and (ii) 38% of the essential genes are associated with lipid metabolism [13]. Several studies have also highlighted that lipid metabolism was elevated in amastigotes when compared with promastigotes [14–16]. Miltefosine, a FDA-approved anti-leishmanial drug is believed to target lipid metabolism of *Leishmania* [17]. Lipid metabolism of *Leishmania* gained lot of attention in the last decade and is of our interest for the discovery of new drug targets [18].

Lipases are one of the key enzymes in lipid metabolism which act on triglycerides and phospholipids of the host. These macromolecules are abundant in mammalian phagolysosomes where lipid-scavenging pathogens reside [19]. Lipases of pathogens have multitude of functions in many pathophysiological processes including virulence, transmission, life cycle development, modulation of host lipids and host immune responses [20–23]. Lipases from human pathogens notably *Mycobacterium tuberculosis*, *Candida albicans*, *Cryptococcus neoformans* and *Malassezia* species are proven for their role in virulence and survival [24,25].

LdLip3, a lipase from *L. donovani*, is believed to participate in key biological processes that include host lipid degradation, alteration

* Corresponding author. Tel.: +91 361 2582213; fax: +91 361 2582249.
E-mail address: sanjukta@iitg.ernet.in (S. Patra).

Table 1
LdLip3 and its homologs used in the multiple sequence alignment study.

UniProtKB accession	Name	Organism	Identity (%)[a]	Similarity (%)[a]
D7P7V3	LdLip3	*L. donovoni*		
A4I6H7	Li-Lip	*L. infantum*	99	99
Q4Q6I0	Lm-Lip	*L. major*	89	91
P19515	Rm-TGL	*R. miehei*	35	45

[a] Identity and similarity of the corresponding protein against LdLip3.

of phagolysosome membrane and structural remodeling of membrane lipids for the survival and infection of pathogen. LdLip3 might favor the parasite growth and development in the host [26]. Hence, LdLip3 could be an attractive drug target to combat leishmaniasis. Targeting LdLip3 of the pathogen is considered as therapeutic strategy in the present study and attempts were made to identify novel potential inhibitors that might preferentially kill *Leishmania*. The three dimensional (3D) model of LdLip3 was predicted which was further utilized for the structure-based drug discovery (SBDD). The similarity-based virtual screening of representative chemical scaffolds was opted for the identification of potential inhibitors [27–29]. Furthermore, the anti-leishmanial activity of the screened hits was validated with experimental assay, resulting in the identification of four novel lead-like molecules. The identified novel anti-leishmanial agents could serve as potential candidates for drug development against leishmaniasis that might address infectious diseases caused by Trypanosomatida protozoans.

2. Materials and methods

2.1. Homology modeling

The protein sequence of LdLip3 (UniProt ID: D7P7V3) and its representative homologs from leishmanial species were collected from UniProtKB (www.uniprot.org). The retrieved sequences were subjected to multiple sequence alignment with ClustalW and subsequently analyzed with ESPript to identify functionally important residues, motifs and protein domains [30,31] (Table 1).

The appropriate template for homology modeling was identified by searching the structural homologs using 'BLASTP' program against Protein Data Bank (PDB). Lipase from *Rhizomucor miehei* (Rm-TGL) in its inhibitor bound conformation (PDB id: 4TGL) was used as template for structure modeling based on its sequence and functional homology [32]. The first 20 residues of LdLip3 were not modeled due to lack of structural information of Rm-TGL. Initially hundred models were generated with MODELLER9v7 which were then ranked on the basis of their discrete optimized protein energy (DOPE) and restraint violation (molpdf) scores [33,34]. The best model having reasonable DOPE and molpdf scores with acceptable statistics with PROCHECK [35] and Errat plot [36] was validated using NIH SAVES server. Protein fold of LdLip3 model was evaluated using knowledge-based energy profile of ProSA program [37,38]. The best model of LdLip3 from structure validation studies was analyzed for stability using GROMOS96 43a1 force field under periodic boundary conditions in GROMACS4.5.5 package [39–41]. The system was solvated with simple point charge (SPC) water model. The net charge of system was neutralized by replacing water molecules that are at least 3.50 angstroms (Å) from the protein surface with four chlorine ions. The system was energy minimized to remove bad contacts using steepest descent algorithm. The solvent was equilibrated for 500 ps in NVT ensemble by restraining the solute atoms through a harmonic force constant of 1000 kJ nm^{-2}. Then the system was equilibrated by restraining all the bonds for 500 ps in NPT ensemble which was followed by 500 ps of equilibration without any restraints. Production run was carried out for 20 ns with NPT

ensemble using 2 fs of integration time. Simulations were carried out with velocity rescaling thermostat at 300 K in which protein and non-protein atoms were coupled to separate temperature coupling baths and pressure was controlled at 1 atm using Parrinello-Rahman barostat. The linear constraint solver (LINCS) algorithm was used to constrain the bonds involving hydrogen atoms [42,43]. Particle Mesh Ewald (PME) summation method was used for calculating the long-range electrostatic interactions with 12 Å cut-off. Conformations of LdLip3 model from the production run were analyzed as time-dependent function to check the conformational stability of energy minimized LdLip3 model in the solvent system.

2.2. Similarity-based virtual screening

2.2.1. Virtual screening

The success of virtual screening in the identification and enrichment of lead and lead-like molecules are well reported [44–48]. Virtual screening of small molecules was performed using the energy minimized model of LdLip3 with AutoDock4.2 using lamarckian genetic algorithm (LGA) [49,50]. NCI diversity set II was used to identify structurally diverse molecular scaffolds that contain 1880 chemical molecules (2654 molecular structures). The choice of NCI diversity set explores the vast chemical space and meanwhile greatly reduces the computational time as it contains only the representative scaffolds and the task can be carried out with limited computational resources. LdLip3 model was preprocessed by adding hydrogen atoms to all the residues followed by addition of Gasteiger-Marsili charges. Then non-polar hydrogen atoms were merged into their respective heavy atoms and atom types were fixed using AutoDockTools [51]. All the small molecules were similarly processed using 'prepare_ligand4' python script available with AutoDockTools distribution. For docking simulations, a grid box of 90 × 90 × 90 points was constructed with grid spacing of 0.375 Å keeping catalytic serine (Ser168) at the center of grid box that covers the entire active site of LdLip3 model. Grid maps were generated for all the atom types present in the grid box along with electrostatic and desolvation maps using the AutoGrid utility. The whole docking procedure was then repeated with the human structural ortholog – monoglyceride lipase (MGL), to find the potential inhibitors that could be effective toward LdLip3 than human MGL (PDB id: 3HJU) [52]. Molecular docking of NCI diversity set was performed with an initial population size of 300 for 20 independent LGA runs. In each run, the best individual from each generation was propagated to the next generation and remaining docking parameters were set to default. Each molecule was clustered on the basis of positional root-mean-square deviation (RMSD) between the docked positions to predict the optimal binding of the molecules with LdLip3.

The ten top hits were chosen as initial data set based upon their difference in binding free energy better than −2 kcal/mol and interactions of the top hits with leishmanial-specific residues of LdLip3 to carry out similarity screening. Similar molecules (tanimoto coefficient > 0.6) of the ten top hits from ZINC and its natural product database resulted in 22,919 molecules including isomers which were collected and preprocessed [53,54]. Similarity-based virtual screening was intended to understand the structure–activity relationships and to identify molecules with better free energy of binding than hits from initial screening. Virtual screening process was repeated with these similar molecules on both LdLip3 model and human MGL with an initial population size of 300 and 20 independent LGA runs with stringent evaluations of 30,000,000. Docking results were visually analyzed with AutoDockTools and PyMOL to understand the docking poses and interactions between the potential inhibitors and LdLip3 [55]. The top twenty hits were re-docked with 100 independent LGA runs to increase the reliability of the docking predictions (reliability test). The best conformation
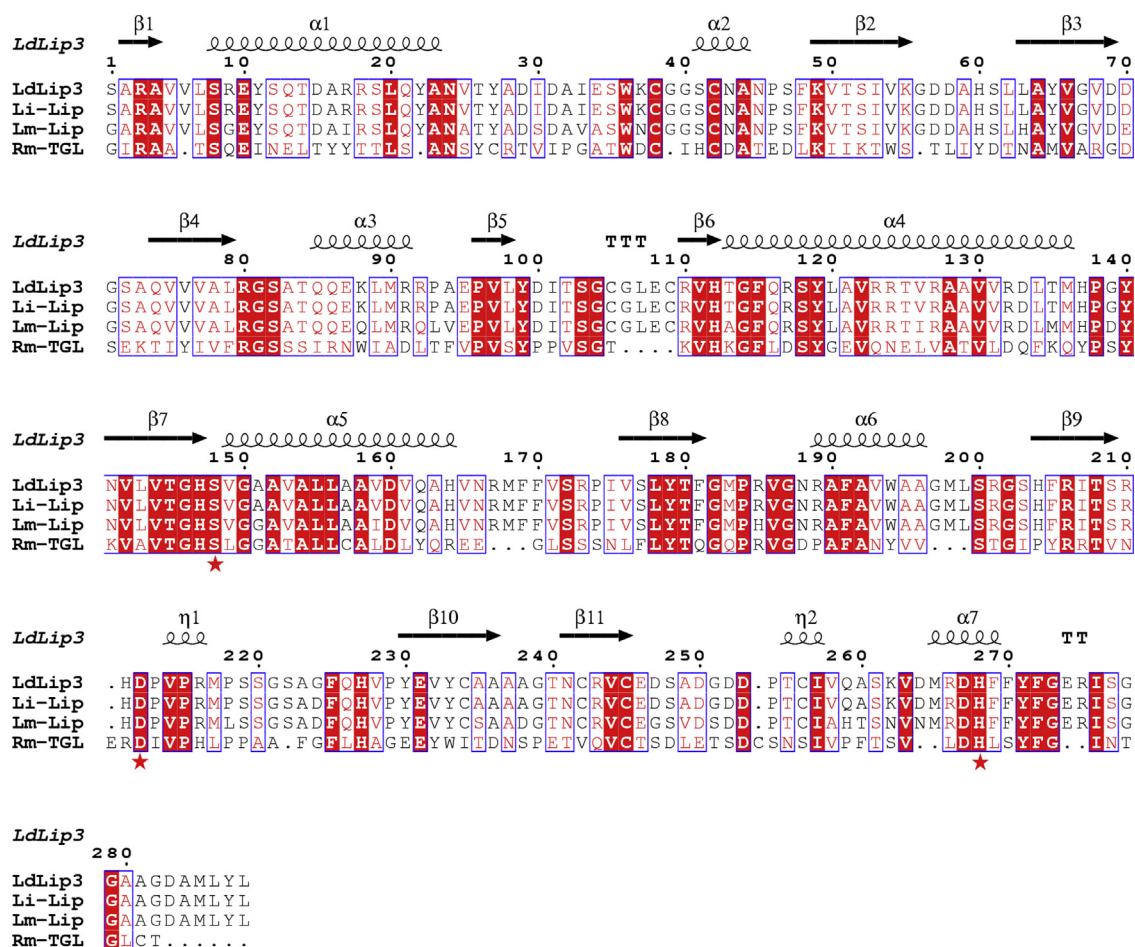
Fig. 1. Multiple sequence alignment of LdLip3 with its homologs. The catalytic resides have been highlighted with star. Numbering of amino acids is denoted with respect to LdLip3. This figure was produced using ESPript.

of the largest cluster from the reliability test was considered as optimal binding conformation of the top twenty hits with LdLip3.

2.2.2. Cluster footprinting analysis

In order to improve the reliability and gather valuable insights from the docking studies, clustering analysis of the docked poses has been carried out on the screened twenty top hits. AuPos-SOM (Automated analysis of poses using self-organizing map) was implemented to identify correct conformations of the hits as well as to discriminate the active hits from the non-active hits from docking studies [56]. AuPosSOM classified the docked poses using ligand–protein contact descriptors followed by unsupervised cluster analysis. Default parameters of AuPosSOM were used while the top hits which have been chosen to carry out *in vivo* studies are considered as active compounds. The top hits were clustered according to the similar binding mode to LdLip3 and generated a Newick tree file which was visualized by Dendroscope. The contact analysis was investigated to determine key interactions and complementarity with the binding site of LdLip3.

2.3. Validation studies of structure-based drug discovery with in vivo assay

2.3.1. Parasites, cell lines and chemicals

The *L. donovani* (BHU-1081) promastigote culture was obtained from Prof. Shyam Sundar, Banaras Hindu University, India and cultivated in M199 liquid media supplemented with 15% heat-inactivated fetal bovine serum (FBS), 100 U/ml penicillin and 100 μg/ml streptomycin. Mouse macrophage cell line J774A.1 used in the study was procured from "National Centre for Cell Science" (NCCS), Pune, India and cultured in RPMI 1640 media supplemented with 10% heat inactivated FBS, 2 mM glutamine, 100 U/ml penicillin and 100 μg/ml streptomycin. The identified top hits with 95% purity were procured from MolPort, Russia based on their availability. All the chemicals used in the experiments were procured from Sigma–Aldrich and Merck.

2.3.2. Anti-leishmanial activity assay

Only four of the screened inhibitors were commercially available. The anti-leishmanial effects of these procured top hits were investigated by optimized MTT (3-(4,5-dimethylthiazol-2-yl)-2,5-diphenyltetrazolium bromide) assay [57–59]. For the assay, test molecules (5 mM in DMSO) serially diluted in media were added to 96-well culture plates with a concentration range of 0.75–100 μm in a total volume of 200 μl. Mouse macrophage cell line J774A.1 were cultured in complete Dulbecco's modified Eagle's medium (DMEM), 2000 cells/well were seeded and were allowed to adhere overnight. 0.5% DMSO served as a negative control, whereas 20% DMSO served as positive control for both parasite and human cell lines. Exponentially growing *L. donovani* promastigotes (2×10^6 cells/ml) were freshly transformed in M199 media and incubated with graded concentrations of compounds at 25 °C for 48 h. After treatment, cells were centrifuged and subsequently washed with $1 \times$ ice-cold phosphate-buffered saline (PBS) and incubated in fresh M199 media with 15% heat-inactivated FBS and 0.5 mg/ml MTT for 4 h. The cell viability was determined by
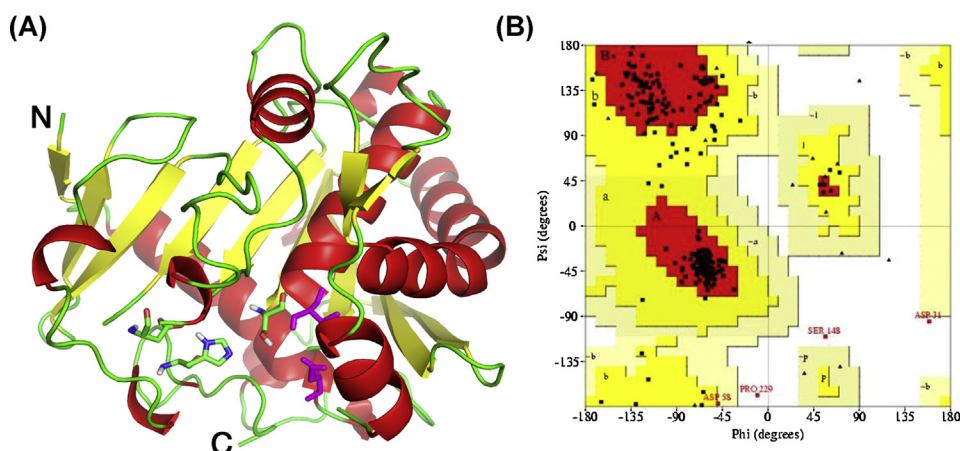
Fig. 2. (A) The 3D model of LdLip3 shown in cartoon representation. Catalytic residues and oxyanion hole (magenta) residues have been shown in sticks. This was produced using PyMOL. (B) Ramachandran plot of LdLip3 revealing the acceptable statistics of dihedral angle distribution of amino acids.

measuring the optical density at 570 nm for reduced formazan, compared to untreated cells. The IC_{50} value for each identified novel inhibitors was calculated by plotting percent cell viability *vs.* concentration.

3. Results and discussion

3.1. Homology modeling

The non-availability of the experimentally determined structure for lipases from pathogenic source hinders the use of structure-based drug discovery approach for several deadly infectious diseases. Homology modeling of LdLip3 was carried out to address the same with the aid of lipase from *R. miehei* in its inhibitor bound conformation (PDB id: 4TGL, resolution: 2.60 Å) to identify potential anti-leishmanial agents. Sequence analysis revealed that LdLip3 is highly conserved throughout the leishmanial species. Conservation between LdLip3 and Rm-TGL is satisfactory in terms of fold and functional residues which is necessary for the reliable LdLip3 model. The catalytic residues were conserved and correspond to Ser168, Asp232 and His288 in LdLip3 (depicted as star in Fig. 1).

The modeled structure confirmed that LdLip3 is a member of serine hydrolases with α/β fold (Fig. 2A). The 3D model of LdLip3 (extends from 21 to 302 residues with 30% identity and 44% similarity toward Rm-TGL) was significantly conserved with leishmanial homologs and Rm-TGL. LdLip3 has α/β hydrolase domain with five-stranded parallel β-sheet covered by two-stranded anti-parallel β-sheet at the N-terminus as shown in Fig. 2A. The nucleophile serine (Ser168) was found at the bend of the tight turn in the 'nucleophilic elbow' and other catalytic residues (Asp232 and His288) are positioned adjacent to each other within the active site. Taken together, structural features of LdLip3 are similar to that of Rm-TGL and other triacylglycerol lipases. Apart from conserved catalytic residues, strict conservation was observed between LdLip3 and Rm-TGL at the active site cavity (4 Å around catalytic residues) namely His167, Gly170, Ala172, Gly202, Pro204, Val234, Pro235, Val283, Asp287 and Tyr291 which might play a role in the enzymatic activity. The residues of oxyanion hole were identified as Ser102 and Val169 which are involved in substrate binding and tetrahedral intermediate stabilization.

The energy minimized structure of LdLip3 model has acceptable statistics of backbone dihedral angle distribution of amino acids in Ramachandran plot with 86.6% in core, 12.2% in additionally allowed and 0.4% in generously allowed region which is comparable with Rm-TGL as presented in Fig. 2B. Along with Asp51 and Pro249, the catalytic nucleophile Ser168 was observed in disallowed region

of Ramachandran plot, a typical feature found in most of the energy minimized serine lipases/esterases. G-factor of LdLip3 was −0.19 which also indicates acceptable statistics of distribution of phi and psi along with chi1, chi2 and chi3 angles (G-factor less than −0.5 is considered to be unusual). Errat plot of LdLip3 showed structural quality of 81.319 with little steric hindrance between few amino acids (Supplementary Fig. 1). As expected, Verify-3D also revealed that 79.86% of the amino acids in the current structure of LdLip3 have compatible 1D-3D score greater than 0.2. The LdLip3 model has *Z*-score of −5.97 is in the range of native conformations of crystal structures with ProSA-web. The fold quality of LdLip3 from ProSA was comparable with experimentally determined Rm-TGL (*Z*-score: −7.01) indicating the acceptability of the modeled LdLip3 structure (Supplementary Fig. 2). Molecular dynamics (MD) was carried out to assess stability of the energy-minimized LdLip3 model to ensure its reliability for similarity-based virtual screening. Time evolution of RMSD of the backbone Cα atoms of LdLip3 showed that it undergoes a significant change in the initial 5 ns of simulations and converged with fluctuations less than 0.1 Å thus indicating stable conformation of LdLip3 model (Supplementary Fig. 3). MD simulations suggested that the energy-minimized LdLip3 model is satisfactory for virtual screening process.

Structural comparison of the energy minimized LdLip3 model with Rm-TGL on Cα-backbone atoms (161 out of 219 aligned atoms) shows overall RMSD of 0.176 Å which was carried out with PyMOL. Structural comparison also reveals that the catalytic site
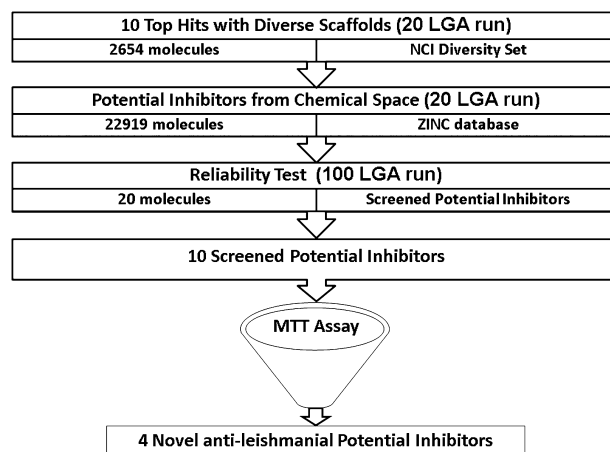

Fig. 3. Flow chart of the similarity-based virtual screening used to identify the potential inhibitors that might specifically kill leishmanial cells.

of LdLip3 (9 out of 12 Cα-backbone atoms around 4 Å of catalytic residues with RMSD of 0.337 Å) is similar to Rm-TGL and residues Arg38, Ser102, Arg111, Met285 and Arg286 in LdLip3 were exclusively found in the catalytic site. The leishmanial-specific residues at the catalytic pocket have been exploited to screen potential leishmanial-specific lipase inhibitors.

3.2. Similarity-based virtual screening

Similarity-based virtual screening was used to identify potential inhibitors using LdLip3 modeled structure in a step-wise manner utilizing NCI diversity set followed by small molecules from ZINC database including natural products (Fig. 3). The methodology has been validated and implemented successfully for identification of potential inhibitors to combat tuberculosis [60,61]. The rigid docking protocol of AutoDock was utilized for virtual screening keeping protein as rigid and ligand as flexible [62]. In our earlier studies, docking protocol was validated for lipases with help of human MGL [60]. Human MGL was considered as the anti-target from the human proteome for the present study.

Since the structural features required for its inhibition is not yet known, the active site of LdLip3 was considered to screen structurally diverse molecules (NCI diversity dataset II) to identify potential inhibitors with different scaffolds. Screening of diversity set was initially carried out against human MGL to reduce the possibility of potential inhibitors inhibiting human MGL. The molecules with higher binding affinity toward LdLip3 than human MGL (based on the difference in predicted free energy of binding) were considered as the top hits of initial screening (Supplementary Table 2). Subsequently, similarity screening of the ten top hits from initial screening was carried out on ZINC and its natural product database to identify potential inhibitors that could be

Table 2
The twenty top hits identified from similarity-based virtual screening. Number of conformations in largest cluster is given in parenthesis.

S. No.	Molecule	Free energy of binding (kcal/mol)		
		LdLip3	Human MGL	Difference
	ZINC04701128	−9.23 (51)	−6.00 (18)	−3.23
	ZINC04008765*	−8.83 (93)	−6.11 (25)	−2.72
	ZINC13409341	−8.33 (87)	−5.66 (29)	−2.67
	ZINC01821375*	−9.78 (61)	−7.18 (15)	−2.6
	ZINC13997735	−9.19 (100)	−6.64 (61)	−2.55
	ZINC06117316*	−8.60 (100)	−6.19 (15)	−2.41
	ZINC12653571*	−8.60 (84)	−6.43 (46)	−2.17
	ZINC47367575	−9.76 (64)	−7.60 (29)	−2.16
	ZINC13406344	−8.51 (91)	−6.38 (24)	−2.13
	ZINC18707267	−10.37 (50)	−8.35 (29)	−2.02
	ZINC00472657	−9.78 (30)	−7.70 (52)	−2.08
	ZINC01165396	−10.04 (41)	−7.94 (39)	−2.1
	ZINC01609336	−9.32 (40)	−7.38 (11)	−1.94
	ZINC02141591	−10.26 (22)	−7.55 (20)	−2.71
	ZINC02873758	−9.60 (23)	−7.49 (12)	−2.11
	ZINC03844930	−9.81 (32)	−6.93 (13)	−2.88
	ZINC04280995	−9.46 (33)	−6.33 (8)	−3.13
	ZINC05260149	−9.55 (48)	−7.30 (35)	−2.25
	ZINC07053328	−10.28 (22)	−8.22 (36)	−2.06
	ZINC12296526	−8.35 (37)	−7.54 (22)	−0.81

selective toward LdLip3. Top hits of computational studies were visually inspected and analyzed for all possible hydrogen bond and hydrophobic interactions with LdLip3 using PyMOL. The twenty top hits of similarity screening are listed in Table 2. The contact analysis of the top hits was studied with LdLip3 and compared with Lm-Lip, Rm-TGL and Human MGL. The non-conserved amino acids of LdLip3 in contact with the top hits might lead to the specific inhibition of LdLip3 (Supplementary Table 3).
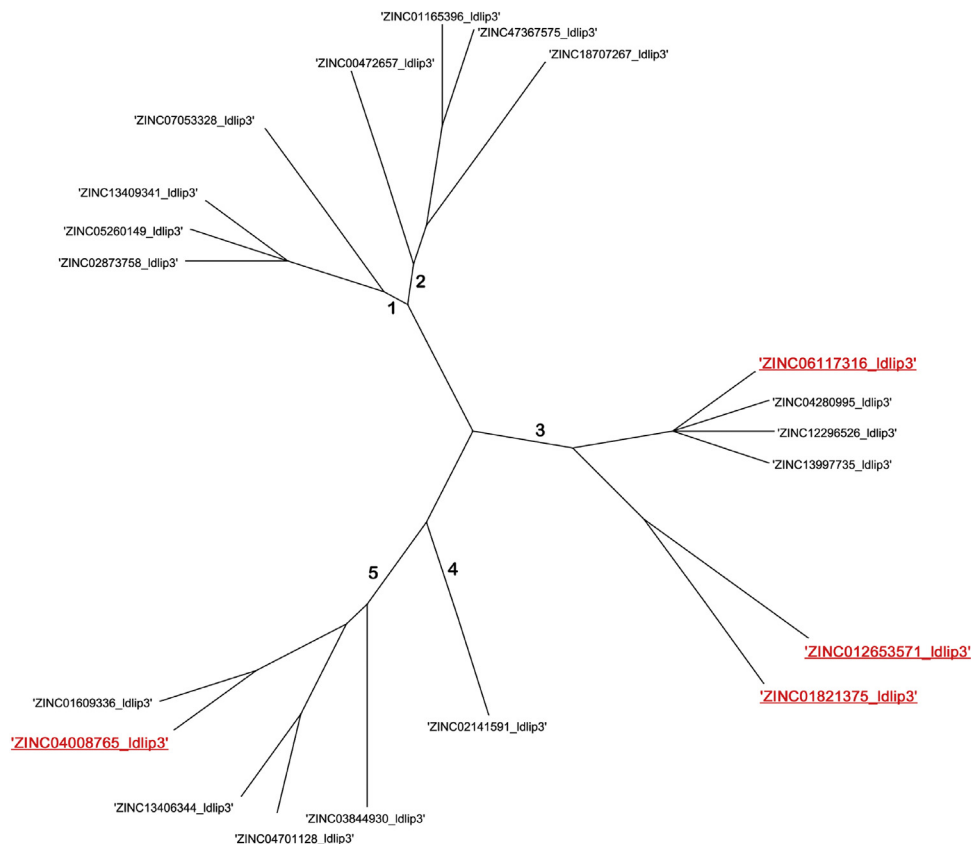

Fig. 4. Tree representation of contact footprints clustering for 20 screened hits with LdLip3. Numbers on branches represent each of the five clusters with ZINC database id of each screened hits. The top hits screened for *in vivo* assay are represented in bold.

Table 3

Conserved contacts of screened twenty top hits at the ligand binding pocket of LdLip3 within clusters and various sub-clusters in each cluster, and screened hits belonging to the sub-cluster.

Cluster	Contact residues conserved within cluster	Hydrogen bond interactions conserved with LdLip3	Sub-cluster [ZINC database id of molecules]	contact residues conserved within sub-cluster	Hydrogen bond interactions within sub-cluster
1	Lys108, Arg111, Arg112, Ala114, His132, Phe135, Ser168, Pro204, Val234, Met237, Pro238	Arg111[HE], Arg111[HH21]	1. [ZINC13409341, ZINC02873758, ZINC05260149] 2. [ZINC07053328]		– – – –
2	Lys108, Arg111, Arg112, Ala114, His132, Phe135, Pro204, Val234, Met237, Pro238		1. [ZINC00472657] 2. [ZINC01165396, ZINC47367575] 3. [ZINC18707267]	Pro93	Arg111[HE], Arg111[HH21], Arg111[O] – – Arg111[HE], Arg111[HH21], Arg112[O]
3	Lys108, Arg111, Arg112, Met237	Arg111[HH21]	1. [ZINC04280995, ZINC06117316[a], ZINC12296526, ZINC13997735] 2. [ZINC01821375[a], ZINC12653571[a]]	His112, Phe115, Pro184, Pro218	– – – – Arg111[HE] –
4	Lys108, Arg111, Arg112, Ala114, His132, Phe135, Ser168, Pro204, Val234, Met237, Pro238	Arg111[HE], Arg111[HH21]	1. [ZINC02141591]		– –
5	Lys108, Arg111, Arg112, Phe135, Pro204, Val234, Met237, Pro238	Arg111[HE], Arg111[HH21]	1. [ZINC03844930] 2. [ZINC04701128, ZINC13406344] 3. [ZINC01609336, ZINC04008765[a]]	Ala94, His112 Ala94, His112,	Arg112[HH11] – – – –

[a] The potential inhibitors that were validated by MTT assay.

3.2.1. Contact footprinting through clustering analysis of docked poses from screened hits

Contact-based clustering using the docking poses which has been investigated can provide insight on the binding mode of small molecules with the protein of interest. The screened hits were clustered into 5 clusters which have been investigated at the level of sub-clusters to discriminate the contacts of each sub-cluster (Fig. 4). Clustering revealed that the top hits were clustered based on the possible interactions as well as the contacts with LdLip3 according to the orientation of the top hits at the active site of LdLip3. The sub-clusters observed within the clusters showed the minor variation in the mode of hydrogen bond interactions (Table 3).

The screened hits from similarity screening were prioritized with set of customized parameters to increase the reliability of the docking studies: (a) number of conformations in the largest cluster for LdLip3 was set to be more than 50 and (b) difference between the free energy of binding between LdLip3 and human MGL was set to be less than 2 kcal/mol. The screened potential inhibitors from SBDD have been listed in Table 4.

Comparative analysis of the top hits with the substrate as well as the inhibitors of human MGL reveals that the top hits bind well with LdLip3 and could be effective against LdLip3. The differences in the 'lid' region which covers the catalytic triad between LdLip3 and human MGL give rise to different binding modes of top hits.
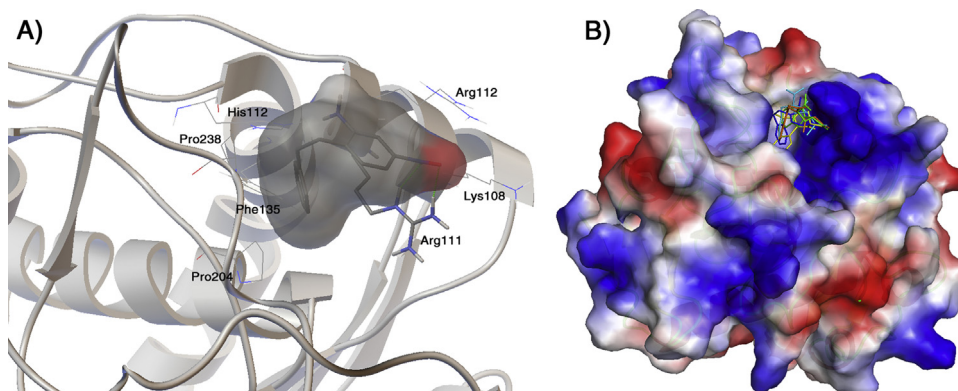

Fig. 5. (A) Hydrogen bond interactions of LdLip3 and the best hit ZINC04701128 predicted by docking studies. (B) Top Hits interact with the leishmanial-specific residue Arg111 in the active site pocket of LdLip3.

Table 4

The screened potential inhibitors from SBDD study. Number of conformations of top hits in cluster with best binding energy of LdLip3 and human MGL is given in parenthesis. Hydrogen bond interactions were predicted with AutoDockTools. Atoms of the residues involved in hydrogen bonds have been indicated in the square brackets.
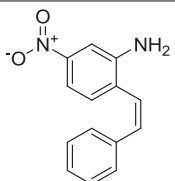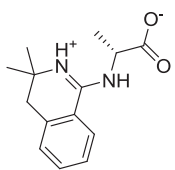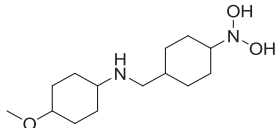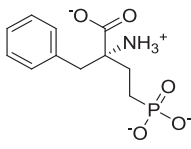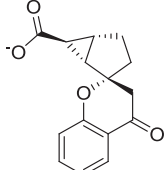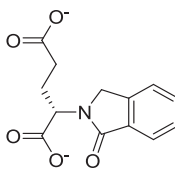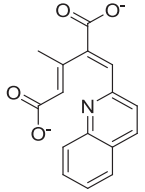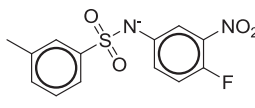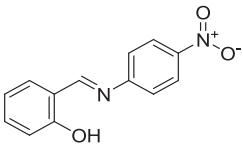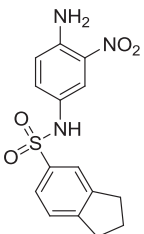
S. No.	Molecule	Free energy of binding (kcal/mol)			Residues forming hydrogen bond
		LdLip3	Human MGL	Difference	
1.	ZINC04701128	−9.23 (51)	−6.00 (18)	−3.23	Arg111[HE], Arg111[HH21]
2.	ZINC04008765*	−8.83 (93)	−6.11 (25)	−2.72	Arg111[HE], Arg111[HH21]
3.	ZINC13409341	−8.33 (87)	−5.66 (29)	−2.67	Arg111[HE], Arg111[HH21]
4.	ZINC01821375*	−9.78 (61)	−7.18 (15)	−2.6	Arg111[HE], Arg111[HH21]
5.	ZINC13997735	−9.19 (100)	−6.64 (61)	−2.55	Arg111[HE], Arg111[HH21],
6.	ZINC06117316*	−8.60 (100)	−6.19 (15)	−2.41	Arg111[HE], Arg111[HH21], Arg112[HH12], Arg112[HH22]
7.	ZINC12653571*	−8.60 (84)	−6.43 (46)	−2.17	Arg111[HE], Arg111[HH21], Arg111[HH22]
8.	ZINC47367575	−9.76 (64)	−7.60 (29)	−2.16	Arg111[HE], Arg111[HH21]

Table 4 (*Continued*)

S. No.	Molecule	Free energy of binding (kcal/mol)			Residues forming hydrogen bond
		LdLip3	Human MGL	Difference	
9.	ZINC13406344	−8.51 (91)	−6.38 (24)	−2.13	Arg111[O], Arg111[HE], Arg111[HH21]
10.	ZINC18707267	−10.37 (50)	−8.35 (29)	−2.02	Arg111[HE], Arg111[HH21], Arg112[O]
Substrate	4-Lumbelliferyl stearate	−6.5 (9)	−8.9 (4)	2.40	nil
Inhibitor	Orlistat	−4 (7)	−7.64 (2)	−0.64	Arg111[2]
Inhibitor	ZYH	−7.27 (66)	−11.14 (46)	3.87	nil

* The potential inhibitors which were validated by MTT assay.

Differences in the residues comprising binding pockets of the top hits in LdLip3 were exploited in the identification of potential inhibitors that makes them preferential toward LdLip3 than human MGL. Best hit ZINC04701128 forms two hydrogen bond interactions with side-chain atoms of Arg111 (Fig. 5). Most of the top hits form hydrogen bonds with Arg111 and Arg112. The interaction mode of the screened molecules which were selected for experimental validation has been shown in Fig. 6. The polar moiety of top hits interacts well with the polar amino acids of LdLip3 notably Lys108, Arg111, Arg112 which is not present in human MGL. The ring
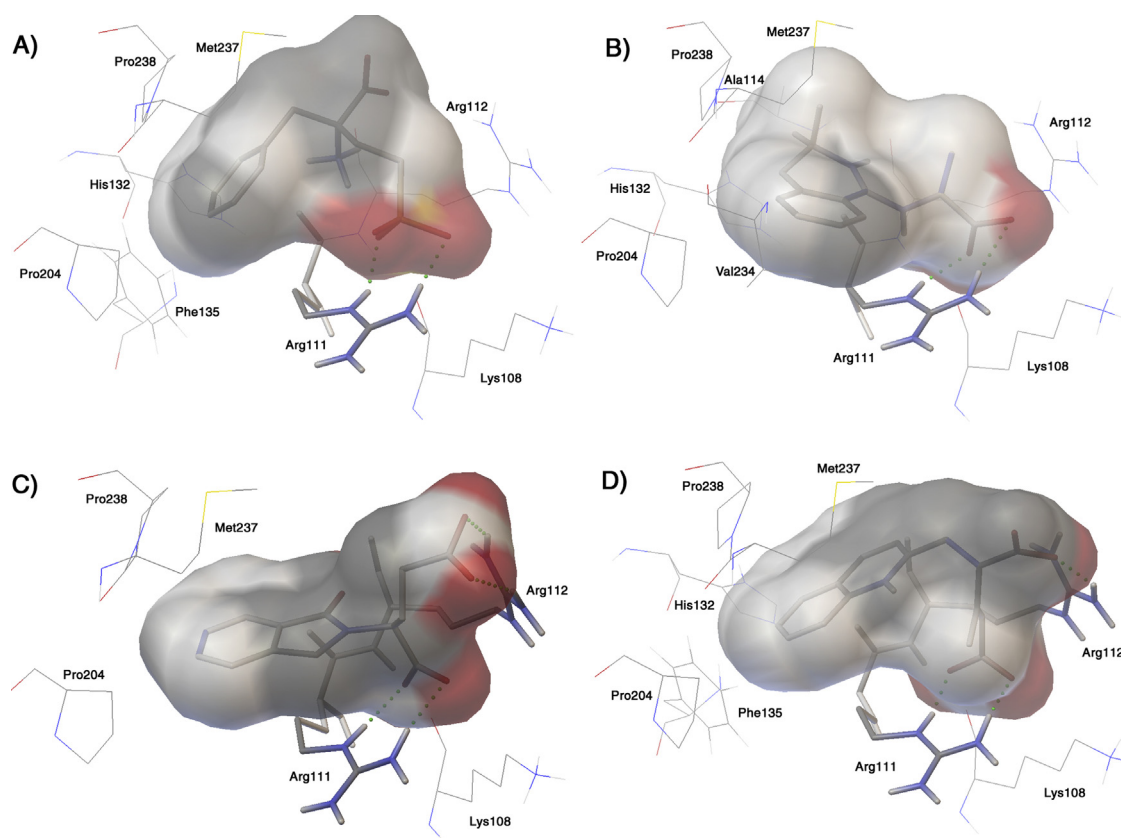

Fig. 6. Hydrogen bond interactions in the active site pocket of LdLip3 with the screened molecules (A) ZINC01821375, (B) ZINC04008765, (C) ZINC06117316 and (D) ZINC12653571.
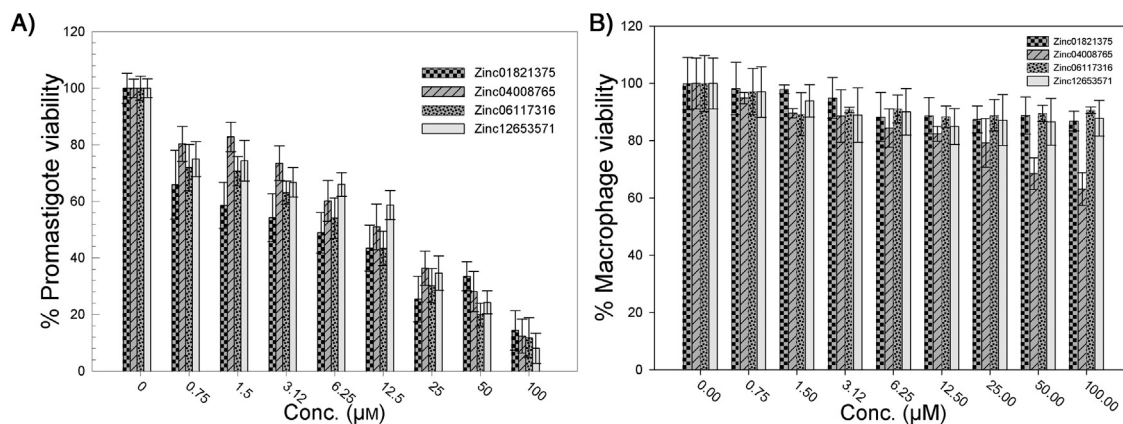
Fig. 7. MTT cell proliferation assay showing promising anti-leishmanial activity of the commercial available potential inhibitors in a dose-dependent manner. (A) Effect of the identified novel inhibitors on *L. donovani* promastigotes. (B) Effect of the identified novel inhibitors on mouse macrophage cell line. Values are mean ± SD of four determinations.
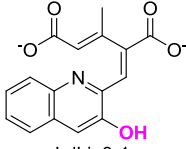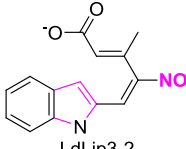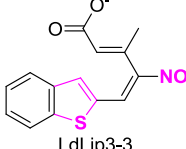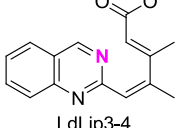
moiety of top hits helps in stabilizing them in the hydrophobic pocket of LdLip3 notably Ala114, Phe115, Val169, Val234, Met237, Val283.

3.3. Anti-leishmanial activity of the screened molecules

The anti-leishmanial activity of procured potential inhibitors (commercially available four molecules) from the screened hits was evaluated by MTT assay (Fig. 7). A dose-dependent death profile of *L. donovani* (BHU-1081 strain) promastigote cells was observed with all the tested molecules in the range of 0.75–100 μM. The molecules ZINC01821375 and ZINC06117316 were more effective as

anti-leishmanial compared to ZINC04008765 and ZINC12653571. The IC_{50} values for each of the molecules were calculated by plotting viable promastigotes in percentage *vs.* concentration. The IC_{50} were found to be 5.2 ± 1.8 μM for ZINC01821375, 13.1 ± 2.6 μM for ZINC04008765, 9.4 ± 2.6 μM for ZINC06117316 and 17.3 ± 3.1 μM for ZINC12653571. The experimentally determined IC_{50} of identified anti-leishmanial agents are concurrent with free energy of binding predicted by docking except ZINC06117316. Molecule ZINC06117316 exhibited better IC_{50} than docking which might be due to the better occupancy of charged alkyl chain in the binding pocket of LdLip3 due to its inherent stereoisomerism. In addition, the effect of identified anti-leishmanial agents on mouse

Table 5

The new molecules designed based on SBDD and *in vivo* studies. Number of conformations of top hits in cluster with best binding energy of LdLip3 and human MGL is given in parenthesis. Hydrogen bond interactions were predicted with AutoDockTools. Atoms of the residues involved in hydrogen bonds have been indicated in the square brackets.

S. No.	Molecule[a]	Free energy of binding (kcal/mol)			Residues forming hydrogen bond
		LdLip3	Human MGL	Difference	
1.	LdLip3-1	−11.67 (68)	−8.36 (32)	−3.31	Arg111[O], Arg111[HH21], Arg112[HH11]
2.	LdLip3-2	−9.93 (78)	−7.35 (24)	−2.58	Arg111[O], Arg111[HH21], Arg112[HH12]
3.	LdLip3-3	−9.57 (85)	−7.13 (18)	−2.44	Arg111[HE], Arg111[HH21], Arg112[HH12]
5.	LdLip3-4	−9.17 (78)	−6.88 (13)	−2.29	Arg111[HE], Arg111[HH21], Arg112[HH12]

[a] The inclusion/replacement of functional group on the top hits are depicted with magenta color.
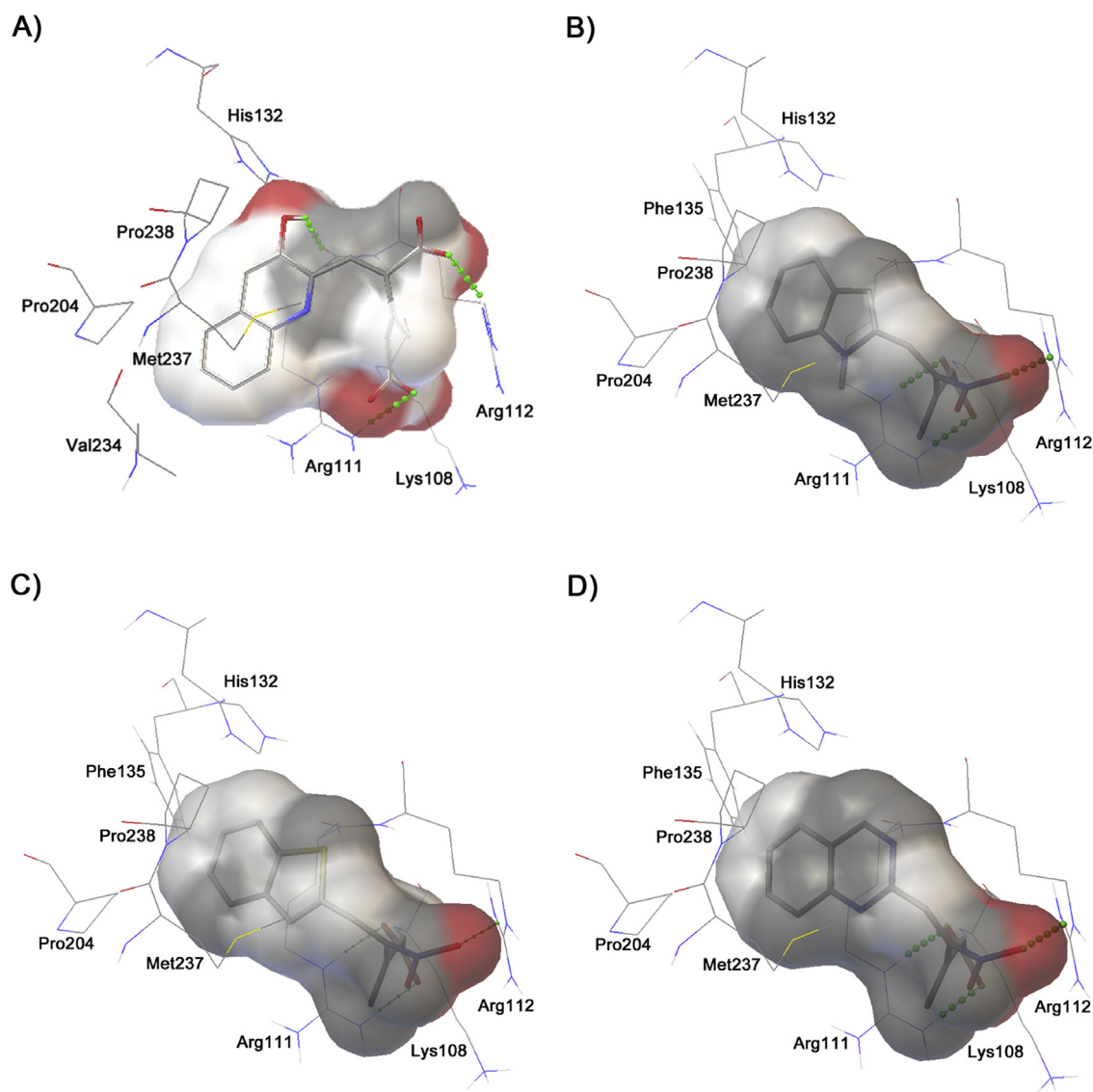
Fig. 8. Hydrogen bond interactions in the active site pocket of LdLip3 with the designed molecules (A) LdLip3-1, (B) LdLip3-2, (C) LdLip3-3 and (D) LdLip3-4.

macrophage cell line J774A.1 was also tested. No significant toxicity was shown on the macrophage cells even at higher concentration up to 100 μM, indicating the identified novel anti-leishmanial agents selectively inhibit leishmanial cells.

3.4. Design of new molecules

Contact footprinting analysis from SBDD provided insights on the binding mode of interaction between the best hits with LdLip3 which showed the path to design new molecules with improved free energy of binding than discovered anti-leishmanial agents. Visual inspection of the binding mode concurrent with contact footprinting of discovered anti-leishmanial agents revealed the presence of polar amino acids in their purlieu. Functional modification of discovered anti-leishmanial agents that favor ionic interactions are possible candidates for the design of new molecules which are accomplished by incorporation of NH_2, NO_2 and OH groups in the molecules of interest.

The detailed information of new molecules is summarized in Table 5 and Fig. 8. The NH_2, NO_2 and OH have been incorporated in the quinolone ring in the 'meta' position relative to the nitrogen atom. As expected, the incorporation of OH group improvised

the free energy of binding of the new molecule (increase in free energy of binding by −3.07 kcal/mol). The change in conformation of binding mode was observed with the incorporation of hydroxy group which leads to the formation of hydrogen bond with leishmanial-specific residue Arg112. Replacement of the six-membered ring with five-membered ring as well as carboxyl group with NO_2 group avoided steric clashes and improved the efficiency of the new molecules in terms of predicted free energy of binding. The study provides insight on the design of lead molecules which could be effective new anti-leishmanial agents.

4. Conclusions

The present work reports LdLip3 lipase as a target enzyme toward leishmaniasis therapeutics. The modeled structure of LdLip3 has been deposited in protein model database with accession number PM0078869 (www.mi.caspur.it/PMDB). The discovery of novel inhibitors against LdLip3 lipase by structure-based drug discovery approach was carried out. Our results suggest that the potential inhibitors bind at the entrance of LdLip3 active site, notably forms hydrogen bond with the leishmanial-specific residue Arg111. The interaction modes of potential inhibitors restrain the

critical 'Lid' region which might result in the inhibition of LdLip3. Contact footprinting analysis revealed that the top hits interact with leishmanial specific residues that might lead to preferential inhibition of LdLip3 than human MGL. The anti-leishmanial activity of the four screened molecules (ZINC01821375, ZINC06117316, ZINC04008765 and ZINC12653571) was validated through MTT assay in promastigote leishmanial cells. The screened molecules had anti-leishmanial activity with IC_{50} (% viable promastigotes vs. concentration) of $5.2 \pm 1.8 \,\mu M$, $13.1 \pm 2.6 \,\mu M$, $9.4 \pm 2.6 \,\mu M$ and $17.3 \pm 3.1 \,\mu M$ for ZINC01821375, ZINC04008765, ZINC06117316 and ZINC12653571, respectively. The screened molecules showed negligible toxicity in mouse macrophage and therefore, highly selective toward the pathogen. Integration of computational and experimental analysis provides valuable insights on the discovered potential inhibitors lead to design of new molecules against LdLip3. Through incorporation of NH_2, NO_2 and OH groups, the designed molecules favored additional ionic interactions with LdLip3 with improvised free energy of binding. Discovered anti-leishmanial agents would serve as starting arsenal to design novel and effective leads to combat leishmaniasis.

Competing interests

None declared

Ethical approval

Not required

Acknowledgements

Appendix A. Supplementary data

Supplementary data associated with this article can be found, in the online version, at http://dx.doi.org/10.1016/j.jmgm. 2014.01.007.

References

[1] World Health Organization, Control of the leishmaniasis: Report of a meeting of the WHO Expert Committee on the Control of Leishmaniasis, Geneva, 22–26 March 2010, WHO Technical Report Series, no. 949, World Health Organization, Geneva, 2010.

[2] P. Desjeux, Leishmaniasis: current situation and new perspectives, Comp. Immunol. Microbiol. Infect. Dis. 27 (2004) 305–318.

[3] C.R. Davies, P. Kaye, S.L. Croft, S. Sundar, Leishmaniasis: new approaches to disease control, Br. Med. J. 326 (2003) 377–382.

[4] A. Clem, A current perspective on leishmaniasis, J. Glob. Infect. Dis. 2 (2010) 124–126.

[5] J. Alvar, I.D. Veílez, C. Bern, M. Herrero, P. Desjeux, J. Cano, J. Jannin, M. den Boer, WHO Leishmaniasis Control Team, Leishmaniasis Worldwide and Global Estimates of Its Incidence, PLoS One 7 (2012) e35671.

[6] J. Alvar, P. Aparicio, A. Aseffa, M. Den Boer, C. Cañavate, J.P. Dedet, L. Gradoni, R. Ter Horst, R. López-Vélez, J. Moreno, The relationship between leishmaniasis and AIDS: the second 10 years, Clin. Microbiol. Rev. 21 (2008) 334–359.

[7] J. Chakravarty, S. Sundar, Drug resistance in leishmaniasis, J. Glob. Infect. Dis. 2 (2010) 167–176.

[8] B. Chawla, R. Madhubala, Drug targets in Leishmania, J. Parasit. Dis. 341 (2010) 1–13.

[9] A.K. Shukla, B.K. Singh, S. Patra, V.K. Dubey, Rational approaches for drug designing against leishmaniasis, Appl. Biochem. Biotechnol. 160 (2010) 2208–2218.

[10] F. Chappuis, S. Sundar, A. Hailu, H. Ghalib, S. Rijal, R.W. Peeling, J. Alvar, M. Boelaert, Visceral leishmaniasis: what are the needs for diagnosis, treatment and control? Nat. Rev. Microbiol. 5 (2007) 873–882.

[11] T.K. Smith, T.B. Reynolds, P.W. Denny, Lipid metabolism as a therapeutic target, Biochem. Res. Int. 2012 (2012) e158139.

[12] R.C.N. Melo, A.M. Dvorak, Lipid body–phagosome interaction in macrophages during infectious diseases: host defense or pathogen survival strategy? PLoS Pathog. 8 (2012) e1002729.

[13] M.J. McConville, T. Naderer, Metabolic pathways required for the intracellular survival of Leishmania, Annu. Rev. Microbiol. 6 (2011) 543–561.

[14] D. Rosenzweig, D. Smith, F. Opperdoes, S. Stern, R.W. Olafson, D. Zilberstein, Retooling Leishmania metabolism: from sand fly gut to human macrophage, FASEB J. 22 (2008) 590–602.

[15] T. Naderer, M.J. McConville, The Leishmania–macrophage interaction: a metabolic perspective, Cell. Microbiol. 10 (2008) 301–308.

[16] A.G.M. Tielens, J.J. van Hellemond, Surprising variety in energy metabolism within Trypanosomatidae, Trends Parasitol. 25 (2009) 482–490.

[17] M. Rakotomanga, S. Blanc, K. Gaudin, P. Chaminade, P.M. Loiseau, Miltefosine affects lipid metabolism in Leishmania donovani promastigotes, Antimicrob. Agents Chemother. 51 (2007) 1425–1430.

[18] F.R. Opperdoes, G.H. Coombs, Metabolism of Leishmania: proven and predicted, Trends Parasitol. 23 (2007) 149–158.

[19] M. McConville, D. de Souza, E. Saunders, V.A. Likic, T. Naderer, Living in a phagolysosome; metabolism of Leishmania amastigotes, Trends Parasitol. 23 (2007) 368–374.

[20] F. Stehr, A. Felk, A. Gácser, M. Kretschmar, B. Mähnss, K. Neuber, B. Hube, W. Schäfer, Expression analysis of the Candida albicans lipase gene family during experimental infections and in patient samples, FEMS Yeast Res. 4 (2004) 401–408.

[21] D.G. Russell, B.C. van der Ven, W. Lee, R.B. Abramovitch, M.J. Kim, S. Homolka, S. Niemann, K.H. Rohde, Mycobacterium tuberculosis wears what it eats, Cell Host Microbe 8 (2010) 68–76.

[22] R. Dhouib, F. Laval, F. Carrière, M. Daffé, S. Canaan, A monoacylglycerol lipase from Mycobacterium smegmatis involved in the bacterial cell interaction, J. Bacteriol. 192 (2010) 4776–4785.

[23] N.P. West, K.M. Cergol, M. Xue, E.J. Randall, W.J. Britton, R.J. Payne, Inhibitors of an essential mycobacterial cell wall lipase (Rv3802c) as tuberculosis drug leads, Chem. Commun. (Camb.) 47 (2011) 5166–5168.

[24] G. Singh, G. Singh, D. Jadeja, J. Kaur, Lipid hydrolizing enzymes in virulence: mycobacterium tuberculosis as a model system, Crit. Rev. Microbiol. 36 (2010) 259–269.

[25] M. Park, E. Do, W.H. Jung, Lipolytic enzymes involved in the virulence of human pathogenic fungi, Mycobiology 41 (2013) 67–72.

[26] A.M. Shakarian, G.C. McGugan, M.B. Joshi, M. Stromberg, L. Bowers, C. Ganim, J. Barowski, D.M. Dwyer, Identification, characterization, and expression of a unique secretory lipase from the human pathogen Leishmania donovani, Mol. Cell. Biochem. 341 (2010) 17–31.

[27] Y. Tanrikulu, B. Krüger, E. Proschak, The holistic integration of virtual screening in drug discovery, Drug Discov. Today 18 (2013) 358–364.

[28] J. Shen, J. Jiang, G. Kuang, C. Tan, G. Liu, J. Huang, Y. Tang, Discovery and structure–activity analysis of selective estrogen receptor modulators via similarity-based virtual screening, Eur. J. Med. Chem. 54 (2012) 188–196.

[29] T.I. Oprea, H. Matter, Integrating virtual screening in lead discovery, Curr. Opin. Chem. Biol. 8 (2004) 349–358.

[30] J.D. Thompson, D.G. Higgins, T.J. Gibson, Clustal W:, Improving the sensitivity of progressive multiple sequence alignment through sequence weighting, position-specific gap penalties and weight matrix choice, Nucleic Acids Res. 22 (1994) 4673–4680.

[31] P. Gouet, E. Courcelle, D.I. Stuart, F. Metoz, ESPript: multiple sequence alignments in PostScript, Bioinformatics 15 (1999) 305–308.

[32] U. Derewenda, A.M. Brzozowski, D.M. Lawson, Z.S. Derewenda, Catalysis at the interface: the anatomy of a conformational change in a triglyceride lipase, Biochemistry 31 (1992) 1532–1541.

[33] M.A. Marti-Renom, A.C. Stuart, A. Fiser, Comparative protein structure modelling of genes and genomes, Annu. Rev. Biophys. Biomol. Struct. 29 (2000) 291–325.

[34] M.Y. Shen, A. Sali, Statistical potential for assessment and prediction of protein structures, Protein Sci. 15 (2006) 2507–2524.

[35] R.A. Laskowski, M.W. MacArthur, D.S. Moss, J.M. Thornton, PROCHECK: a program to check stereo chemical quality of protein structures, J. Appl. Crystallogr. 26 (1993) 283–291.

[36] C. Colovos, T.O. Yeates, Verification of protein structures: patterns of nonbonded interactions, Protein Sci. 2 (1993) 1511–1519.

[37] M.J. Sippl, Recognition of errors in three-dimensional structures of proteins, Proteins Struct. Funct. Gen. 17 (1993) 355–362.

[38] M. Wiederstein, M.J. Sippl, ProSA-web: interactive web service for the recognition of errors in three-dimensional structures of proteins, Nucleic Acids Res. 35 (2007) W407–W410.

[39] H.J.C. Berendsen, D. van der Spoel, R. van Drunen, GROMACS: a message passing parallel molecular dynamics implementation, Comput. Phys. Commun. 91 (1995) 43–56.

[40] D. van der Spoel, E. Lindahl, B. Hess, G. Groenhof, A.E. Mark, H.J.C. Berendsen, GROMACS: fast, flexible, and free, J. Comput. Chem. 26 (2005) 1701–1718.

[41] B. Hess, C. Kutzner, D. van der Spoel, E. Lindahl, GROMACS 4 algorithms for highly efficient, load-balanced, and scalable molecular simulation, J. Chem. Theory Comput. 4 (2008) 435–447.

[42] B. Hess, H. Bekker, H.J.C. Berendsen, J.G.E.M. Fraaije, LINCS: a linear constraint solver for molecular simulations, J. Comput. Chem. 18 (1997) 1463–1472.

[43] B. Hess, P-LINCS: a parallel linear constraint solver for molecular simulation, J. Chem. Theory Comput. 4 (2008) 116–122.

[44] P.D. Lyne, Structure-based virtual screening: an overview, Drug Discov. Today 7 (2002) 1047–1055.

[45] E. Kellenberger, J.Y. Springael, M. Parmentier, M. Hachet-Haas, J.L. Galzi, D. Rognan, Identification of nonpeptide CCR5 receptor agonists by structure-based virtual screening, J. Med. Chem. 50 (2007) 1294–1303.

[46] G. Nicola, C.A. Smith, E. Lucumi, M.R. Kuo, L. Karagyozov, D.A. Fidock, J.C. Sacchettini, R. Abagyan, Discovery of novel inhibitors targeting enoyl-acyl carrier protein reductase in Plasmodium falciparum by structure-based virtual screening, Biochem. Biophys. Res. Commun. 358 (2007) 686–691.

[47] M.T. Khan, O.M. Fuskevag, I. Sylte, Discovery of potent thermolysin inhibitors using structure based virtual screening and binding assays, J. Med. Chem. 52 (2009) 48–61.

[48] C.H. Leung, D.S. Chan, M.H. Kwan, Z. Cheng, C.Y. Wong, G.Y. Zhu, W.F. Fong, D.L. Ma, Structure-based repurposing of FDA-approved drugs as TNF-α inhibitors, ChemMedChem 6 (2011) 765–768.

[49] G.M. Morris, D.S. Goodsell, R.S. Halliday, Automated docking using a lamarckian genetic algorithm and empirical binding free energy function, J. Comput. Chem. 19 (1998) 1639–1662.

[50] S. Cosconati, S. Forli, A.L. Perryman, R. Harris, D.S. Goodsell, A.J. Olson, Virtual screening with AutoDock: theory and practice, Expert Opin. Drug Discov. 5 (2010) 597–607.

[51] G.M. Morris, R. Huey, W. Lindstrom, M.F. Sanner, R.K. Belew, D.S. Goodsell, A.J. Olson, AutoDock4 and AutoDockTools4: automated docking with selective receptor flexibility, J. Comput. Chem. 30 (2009) 2785–2791.

[52] T. Bertrand, F. Augé, J. Houtmann, A. Rak, F. Vallée, V. Mikol, P.F. Berne, N. Michot, D. Cheuret, C. Hoornaert, M. Mathieu, Structural basis for human monoglyceride lipase inhibition, J. Mol. Biol. 396 (2010) 663–673.

[53] J.J. Irwin, B.K. Shoichet, ZINC – a free database of commercially available compounds for virtual screening, J. Chem. Inf. Model 45 (2005) 177–182.

[54] J.J. Irwin, T. Sterling, M.M. Mysinger, E.S. Bolstad, R.G. Coleman, ZINC: a free tool to discover chemistry for biology, J. Chem. Inf. Model 52 (2012) 1757–1768.

[55] W.L. DeLano, The PyMOL Molecular Graphics System, DeLano Scientific, San Carlos, CA, USA, 2002.

[56] G. Bouvier, N. Evrard-Todeschi, J.P. Girault, G. Bertho, Automatic clustering of docking poses in virtual screening process using self-organizing map, Bioinformatics 26 (2010) 53–60.

[57] T. Mosmann, Rapid colorimetric assay for cellular growth and survival: application to proliferation and cytotoxicity assays, J. Immunol. Methods 65 (1983) 55–63.

[58] A.K. Shukla, S. Patra, V.K. Dubey, Evaluation of selected antitumor agents as subversive substrate and potential inhibitor of trypanothione reductase: an alternative approach for chemotherapy of Leishmaniasis, Mol. Cell. Biochem. 352 (2011) 261–270.

[59] P. Saudagar, V.K. Dubey, Cloning expression, characterization and inhibition studies on Trypanothione Synthetase, a drug target enzyme, from *Leishmania donovani*, Biol. Chem. 392 (2011) 1113–1122.

[60] P. Saravanan, V.K. Dubey, S. Patra, Potential Selective Inhibitors against Rv0183 of *Mycobacterium tuberculosis* targeting host lipid metabolism, Chem. Biol. Drug Des. 79 (2012) 1056–1062.

[61] P. Saravanan, H. Avinash, V.K. Dubey, P. Sanjukta, Targeting essential cell wall lipase Rv3802c for potential therapeutics against tuberculosis, J. Mol. Graphics Modell. 38 (2012) 235–242.

[62] S.F. Sousa, P.A. Fernandes, M.J. Ramos, Protein–ligand docking: current status and future challenges, Proteins 65 (2006) 15–26.